Altered temporal correlations in parietal alpha and prefrontal theta oscillations in early-stage Alzheimer disease

Teresa Montez[a,b,1], Simon-Shlomo Poil[c,1], Bethany F. Jones[b], Ilonka Manshanden[b], Jeroen P. A. Verbunt[b,d], Bob W. van Dijk[b,d], Arjen B. Brussaard[c], Arjen van Ooyen[c], Cornelis J. Stam[b], Philip Scheltens[e], and Klaus Linkenkaer-Hansen[c,2]

[a]Institute of Biophysics and Biomedical Engineering, Faculty of Sciences of the University of Lisbon, Campo Grande, 1749-016 Lisbon, Portugal; [b]Department of Clinical Neurophysiology and MEG Centre, VU University Medical Center, PO Box 7057, 1007 MB Amsterdam, The Netherlands; [c]Department of Integrative Neurophysiology, Center for Neurogenomics and Cognitive Research (CNCR), VU University Amsterdam, De Boelelaan 1085, 1081 HV Amsterdam, The Netherlands; [d]Department of Physics and Medical Technology, VU University Medical Center, De Boelelaan 1117, 1081 HV Amsterdam, The Netherlands; and [e]Alzheimer Center and Department of Neurology, VU University Medical Center, PO Box 7057, 1007 MB Amsterdam, The Netherlands

Edited by Nancy J. Kopell, Boston University, Boston, MA, and approved December 12, 2008 (received for review November 19, 2008)

Encoding and retention of information in memory are associated with a sustained increase in the amplitude of neuronal oscillations for up to several seconds. We reasoned that coordination of oscillatory activity over time might be important for memory and, therefore, that the amplitude modulation of oscillations may be abnormal in Alzheimer disease (AD). To test this hypothesis, we measured magnetoencephalography (MEG) during eyes-closed rest in 19 patients diagnosed with early-stage AD and 16 age-matched control subjects and characterized the autocorrelation structure of ongoing oscillations using detrended fluctuation analysis and an analysis of the life- and waiting-time statistics of oscillation bursts. We found that Alzheimer's patients had a strongly reduced incidence of alpha-band oscillation bursts with long life- or waiting-times (< 1 s) over temporo-parietal regions and markedly weaker autocorrelations on long time scales (1–25 seconds). Interestingly, the life- and waiting-times of theta oscillations over medial prefrontal regions were greatly increased. Whereas both temporo-parietal alpha and medial prefrontal theta oscillations are associated with retrieval and retention of information, metabolic and structural deficits in early-stage AD are observed primarily in temporo-parietal areas, suggesting that the enhanced oscillations in medial prefrontal cortex reflect a compensatory mechanism. Together, our results suggest that amplitude modulation of neuronal oscillations is important for cognition and that indices of amplitude dynamics of oscillations may prove useful as neuroimaging biomarkers of early-stage AD.

Alzheimer's disease | magnetoencephalography | neuronal oscillations | resting-state brain activity | temporal correlations

Psychological and neuroimaging data suggest that the brain performs many important functions during rest, such as retrieval and manipulation of information in short-term memory, and problem-solving and planning (1, 2). These resting-state functions may represent an essential aspect of human self-awareness and are susceptible to impairment in brain-related disorders including depression, schizophrenia, and dementia (3).

Neuroimaging has identified anatomical patterns of activity that are remarkably consistent across resting-state experiments, most notably in the precuneus, lateral parietal and medial prefrontal cortices (4, 5). The existence of such a "resting-state network" has been suggested to reflect a "default mode" of brain operation in the absence of goal-directed behavior (6). Coordination of anatomically distributed activity during rest has been studied extensively by computing correlations between neuronal signals from different brain areas (Fig. 1). This approach has revealed aberrant resting-state networks in Alzheimer disease (AD) (7–9) and other disorders (4, 10, 11).

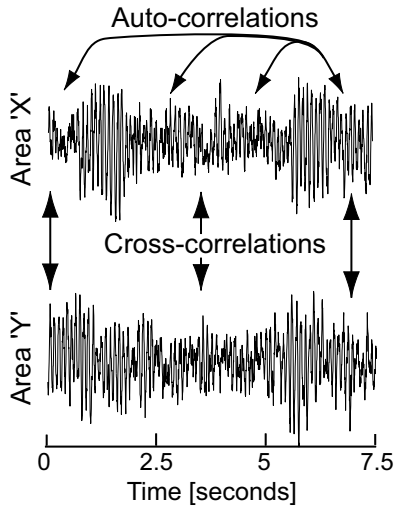

Fig. 1. The study of spatial and temporal dimensions of neuronal processing requires different correlation analyses. Coordination of anatomically distributed activity (parallel processing) may be studied by computing correlations between neuronal signals from different brain areas (*Cross-correlations*). Many different algorithms have been used to detect and quantify the nature of correlations in the spatial domain, e.g., coherence, phase-locking factors, or synchronization likelihood. In contrast, coordination of brain activity over time (serial processing) may be studied by computing autocorrelations in neuronal signals within a single brain area (*Autocorrelations*). Serial processing requires a sequence of causally related neuronal activities, which is likely to give rise to correlations over time (temporal correlations), e.g., persistent oscillatory activity as reflected in a slow amplitude modulation as it is studied here. Thus, by studying autocorrelation properties we may learn more about the mechanisms of attention and memory.

For cognitive processing, coordination of local brain activity over time may be just as important as the coordination of simultaneous activity in anatomically distinct brain regions and may be reflected in the autocorrelation structure of the neuronal

Author contributions: A.B.B., A.v.O., C.J.S., P.S., and K.L.-H. designed the research; B.F.J., I.M., J.P.A.V., B.W.v.D., and P.S. performed research; T.M., S.-S.P., and K.L.-H. analyzed data; and T.M., S.-S.P., A.v.O., C.J.S., P.S., and K.L.-H. wrote the paper.

The authors declare no conflict of interest.

This article is a PNAS Direct Submission.

[1]T.M. and S.S.P. contributed equally to this work.

[2]To whom correspondence should be addressed. E-mail: klaus.linkenkaer@cncr.vu.nl.

This article contains supporting information online at www.pnas.org/cgi/content/full/0811699106/DCSupplemental.

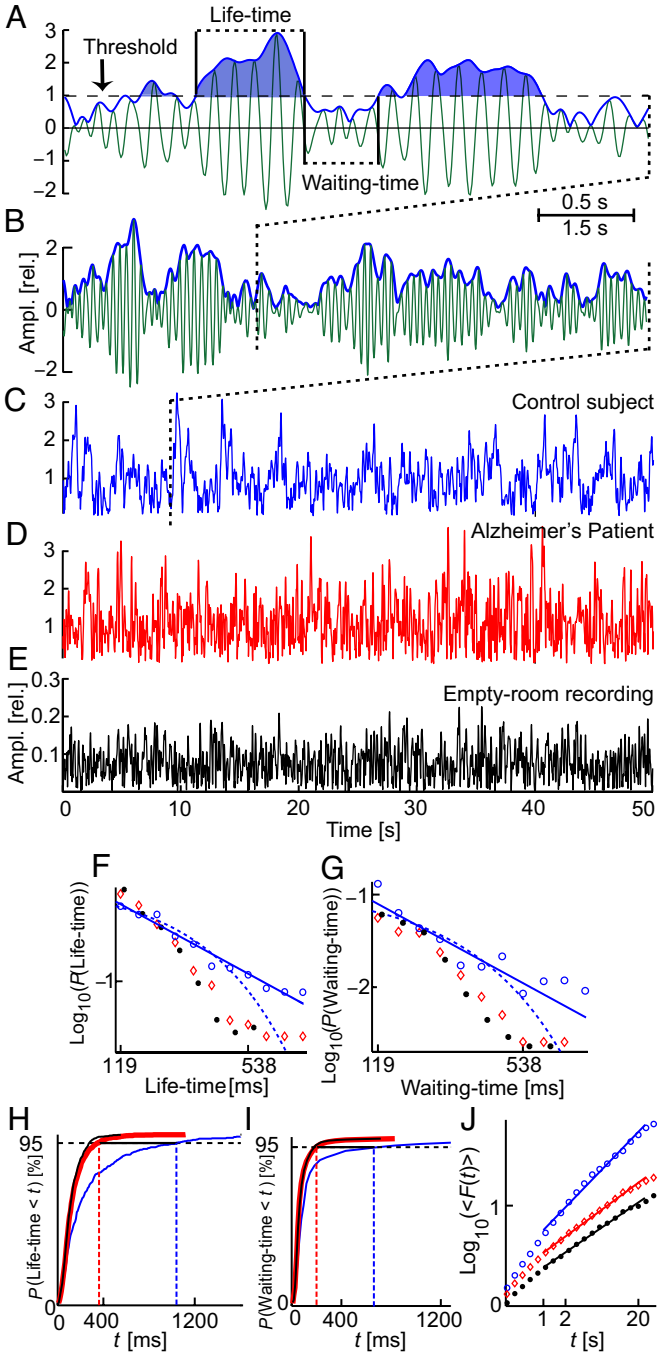

Fig. 2. Three biomarkers for characterizing the amplitude fluctuations of neuronal oscillations. To characterize the amplitude dynamics of ongoing alpha oscillations, the MEG signals were band-pass filtered from 6–13 Hz (*thin green line*) and the amplitude envelope of the oscillations (*thick blue line*) extracted with the Hilbert transform (*A*, *B*). Non-random fluctuations are qualitatively identified as a tendency for oscillations to exhibit amplitude modulations on multiple time scales, as seen in the control subject (*C*), as opposed to rapidly changing amplitude levels even on short time scales, as seen in the AD patient (*D*) and the MEG recording without a subject in the device (*E*). To quantify differences in amplitude dynamics of oscillations on short to intermediate time scales (< 1 s), we introduced a threshold at the median amplitude (*horizontal dashed line* in *A*) and defined the beginning and the end of an oscillation burst as the time points of crossing this threshold. An inherent persistence in the amplitude dynamics on short time scale was reflected in probability distributions of oscillation-burst ''life-times'' and ''waiting-times'' that exhibited power-law–like decays as indicated by the least-squares fit in the double logarithmic plot (*F*, *G*, *straight blue line*), compared with the exponential fit (*F*, *G*, *dashed line*). The probability distributions, however, did not have a sufficiently wide dynamic range to make statistical conclusions about which mathematical function best described the distributions. Instead, we used the 95th percentile of the cumulative probability distributions as an index that captures the fat tail in the distribution of ''life-times'' (*H*) and ''waiting-times'' (*I*) for the AD patient (*thick red line*) and control (*thin blue line*). The DFA exponent provides a quantitative index of the persistence of autocorrelations on longer time scales (1–25 s) and is the slope of the least-square fitted lines in (*J*). The stronger autocorrelations in the control subject (*J*, *blue circles*) compared with the AD patient (*J*, *red diamonds*) is reflected in a DFA exponent closer to 1 (0.81 vs. 0.58). The lack of temporal correlations in (*E*) is reflected in the DFA exponent having the value of ≈0.5, which is characteristic of an uncorrelated random process (*J*, *black dots*). All data were taken from a parietal channel.

signals (Fig. 1). Cognitive functions typically involve a series of operations that require temporal coordination of neuronal activity across many time scales (12, 13). This is true particularly during rest where thoughts unfold on time scales of several seconds and, thus, require ongoing mnemonic activity, such as retrieval, retention, and manipulation of information (11), to ensure continuity and integrity of conscious experiences (3). Interestingly, working-memory studies have recently associated encoding and retention of information with a sustained increase in the oscillation amplitude for several seconds in multiple brain areas and frequency bands, suggesting that a slow modulation of oscillatory activity is an important systems-level mechanism of mnemonic operations (14–16). It remains unknown, however, whether amplitude modulation of local oscillatory activity is impaired in a memory disorder like AD and, therefore, could hold valuable diagnostic and prognostic information (4, 7). The development of objective measures, or so-called "biomarkers," that are sensitive to pathophysiological changes in AD is important for our understanding of the disease, and may enhance our ability to monitor disease progression and provide insights into systems-level mechanisms of mnemonic abilities.

We measured ongoing activity with whole-scalp magnetoencephalography (MEG) in patients diagnosed with early-stage AD and in age-matched control subjects. We quantified the temporal structure of oscillations on short-to-intermediate time scales ($< \approx 1$ s) using cumulative distribution functions of the life- and waiting-times of oscillation bursts. The autocorrelation structure of amplitude fluctuations in ongoing oscillations on long time scales (1–25 s) was characterized using detrended fluctuation analysis (DFA). Our results point to an aberrant autocorrelation structure of temporo-parietal alpha oscillation and medial prefrontal theta activity in early-stage AD.

Results

We measured ongoing activity during eyes-closed rest in patients diagnosed with early-stage AD ($n = 19$) and in age-matched control subjects ($n = 16$) using a 151-channel MEG system. The amplitude envelope of oscillations in the delta, theta, alpha, beta, and gamma bands was extracted using bandpass filters and the Hilbert transform (Fig. 2*A* and *B*) (see *Materials and Methods*). Spectral analysis in the occipito-parietal region revealed that the AD patients had peak frequencies in the range of 6.3–10.0 Hz, which was lower than the age-matched control subjects (7.1–10.7 Hz, $P < 0.05$, two-tailed t test [Fig. S1 *A* and *B*)]. This is in agreement with the well-known slowing of the alpha rhythm in AD (17–19). Thus, to avoid confounding frequency and amplitude effects, we defined the alpha-frequency band to be 6–13 Hz.

To test our hypothesis that the amplitude modulation of local oscillatory activity holds information about pathophysiological changes in early-stage AD, we adopted an ''avalanche analysis'' from the study of critical phenomena to characterize amplitude fluctuations on short to intermediate time scales (< 1 s) (20, 21).

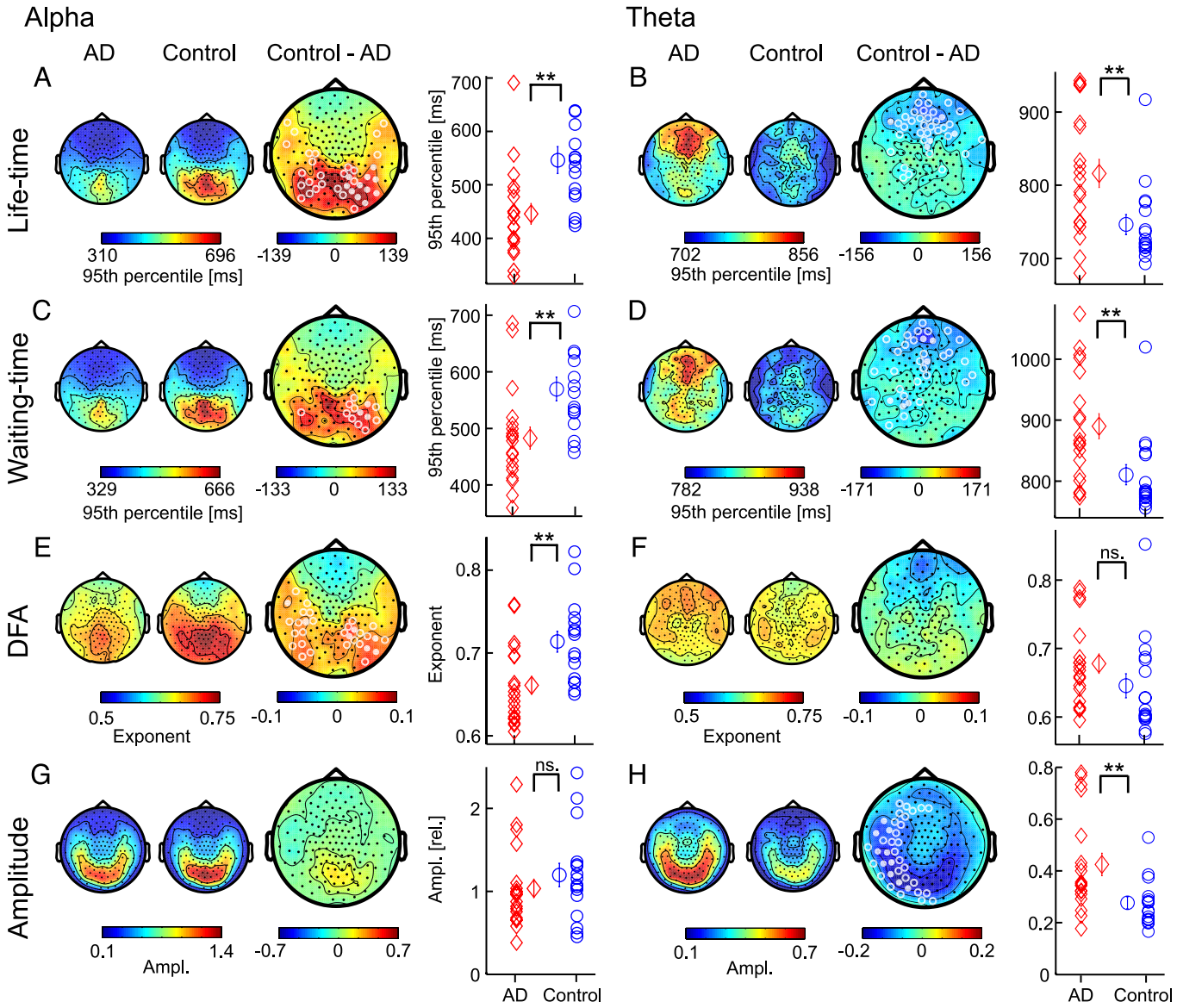

Fig. 3. Aberrant temporal structure of temporo-parietal alpha and medial prefrontal theta oscillations in AD. Grand-average topographies of biomarkers are shown for AD patients (*small left column*), controls (*small middle column*), and controls minus patients (*right column*). Alpha oscillations (6–13 Hz) are shown in the left panel (*A*, *C*, *E*, and *G*) and theta oscillations (4–5 Hz) on the right panel (*B*, *D*, *F*, and *H*). Individual-subject values for the patients (*red diamonds*) and the controls (*blue circles*), and mean ± SEM of the two groups were computed as the average over the channels marked with white circles in the difference topography of a given biomarker. In (*F*) the channels marked in (*B*) were used, and in (G) the average was made across the 12 channels with the largest group difference. White circles denote channels with $P < 0.05$ (*open*), and $P < 0.01$ (*filled*). Each row displays a biomarker: life-time (*A*, *B*), waiting-time (*C*, *D*), DFA exponent (*E*, *F*), and mean amplitude (*G*, *H*).**, group difference at $P < 0.005$; ns (nonsignificant), $P > 0.05$.

We quantified the time periods that oscillations were above and below the median amplitude level in individual channels. These periods are termed oscillation life- and waiting-times, respectively (Fig. 2*A*, see *Materials and Methods*). Visual inspection suggested that the life- and waiting-time probability distributions for the alpha band decayed slowly compared to those of temporally uncorrelated signals that were filtered and analyzed identically to the MEG signals (Fig. 2*F* and *G*; for grand averages see Fig. S1 *C* and *D*). We computed the cumulative probability distributions and extracted the 95th percentile as an index of the probability of oscillations to have long life- or waiting-times in a given location and frequency band (Fig. 2*H* and *I*; for grand averages see Fig. S1 *E* and *F*). These indices are termed "life- and waiting-time biomarkers." We used DFA to quantify the autocorrelation structure on time scales corresponding to multiple oscillation bursts (1–25 s, Fig. 2*C*–*E* and *J*; for grand averages see Fig. S1*G*), because this algorithm has previously been shown to robustly estimate the strength of long-range temporal correlations (22, 23).

The life-time biomarker revealed a lower incidence of long alpha-oscillation bursts over temporo-parietal regions in the patients with 95th percentiles at 446 ± 19 ms in AD and 546 ± 25 ms in controls (Fig. 3*A*; $P < 0.005$, see *Materials and Methods*). This was contrasted by long-lasting theta bursts over medial prefrontal regions in the patients with 95th percentiles at 816 ± 19 ms in AD compared with 746 ± 14 ms in controls (Fig. 3*B*; $P < 0.005$). Interestingly, the same group effects, and also with very similar topographies, were observed with the waiting-time biomarker: parietal alpha oscillations had shorter waiting-times in AD (483 ± 20 ms) than in controls (570 ± 21 ms, Fig. 3*C*; $P <$

0.005), whereas the reverse effect was observed for theta activity mostly in frontal regions (waiting-times of 890 ± 21 ms in AD and 810 ± 17 ms in controls; Fig. 3*D*; $P < 0.005$).

The DFA analysis showed that the lower persistence of temporal correlations in temporo-parietal alpha oscillations in the patients extended to time scales of multiple bursts (Fig. 3*E*, DFA exponents 0.66 ± 0.01 in AD and 0.72 ± 0.01 in the control group, $P < 0.005$), whereas medial prefrontal theta merely exhibited a trend toward stronger correlations as observed on short-to-intermediate time scales (Fig. 3*F*, DFA exponents 0.68 ± 0.01 in AD and 0.65 ± 0.02 in the control group, $P = 0.16$). Note that the MEG data were transformed to planar synthetic gradiometers, which are maximally sensitive to neuronal currents immediately below the sensor (see *Materials and Methods*). The changes in amplitude dynamics are particularly interesting in view of the lack of a group effect on mean amplitude in the alpha band (Fig. 3*G*) and the difference in topography between AD-associated increases in amplitude and in life- and waiting-times in the theta band (Fig. 3*B*, *D*, and *H*). Group differences in DFA, life- and waiting-time biomarkers were not significant in the delta, beta, or gamma bands (Fig. S2 *A*–*C*); however, the control subjects had mean amplitudes that were larger for parietal beta and smaller for left temporo-parietal delta activity compared with those of the patients (Fig. S2*D*).

The tendency of a signal to both stay elevated for relatively long periods and to remain at low levels for long periods is characteristic for a process that is correlated on long time scales (24). It is not trivial, however, that temporal correlations on short-to-intermediate time scales extend to longer time scales (25). Pearson correlation analysis of life- and waiting-time biomarkers vs. DFA revealed a significant linear correlation in the theta band for both groups, but only a significant correlation between the life-time biomarker and DFA in the alpha band (Fig. S3).

Discussion

We have investigated the temporal pattern of ongoing MEG activity at the level of individual sensors and identified an aberrant autocorrelation structure of temporo-parietal alpha and medial prefrontal theta oscillations in early-stage AD. These brain regions have been implicated with mnemonic operations in normal subjects and, especially the temporo-parietal regions, exhibit structural, metabolic, and blood-flow deficits in AD. Taken together with previous electrophysiological data pointing to a sustained increase of parietal alpha and medial prefrontal theta during encoding and retention of information (14–16), our results suggest that amplitude modulation of neuronal oscillations may be important for memory and strongly affected by AD.

The DFA analysis of ongoing oscillations has previously been shown to identify pathophysiological states with spectral and anatomical specificity. In major depressive disorder, temporal correlations were selectively attenuated in the theta band (12), whereas abnormally strong correlations were found near the seizure zone in epilepsy patients, primarily in the beta band (26, 27). Here, we identified a pattern of weaker autocorrelations in alpha oscillations in AD, extending from the parietal region and bilaterally toward the temporal lobes. The life- and waiting-time analysis complemented the DFA in identifying a more random autocorrelation structure of temporo-parietal alpha oscillations on short to intermediate time scales in the patients. This is particularly interesting in view of the insignificant effect of AD on oscillation amplitude in the range of 6–13 Hz, suggesting that the temporal structure is at least as important as the magnitude of the oscillations as a marker of pathophysiology and, possibly, for mnemonic operations. The topographies agree remarkably well with previously identified anatomical regions expressing Alzheimer's associated pathologies based on reductions in blood flow and metabolism during rest (28, 29), cortical atrophy (30), and amyloid deposition (28).

Theta oscillations have also been implicated with working-memory activity, especially in medial prefrontal regions (14, 15, 31), which are also part of the "default resting-state network" (6). Medial prefrontal cortex is also a prominent target of AD, however, mostly in later stages (28–30). In fact, several studies have provided evidence for an increased recruitment of frontal regions, possibly to compensate for structural and functional changes elsewhere in the brain [for a review, see (28)]. We identified a prominent increase in short-to-intermediate time-scale, autocorrelated activity in medial prefrontal theta activity in the AD patients, which is in sharp contrast to the weaker correlations in temporo-parietal alpha. In line with previous neuroimaging studies, we speculate that the frontal increase reflects a compensatory response to maintain memory performance during the initial stages of disease.

It is increasingly being recognized that resting-state activity in neurocognitive networks have a multiscale spatiotemporal structure (32–34). We have previously proposed that the amplitude modulation of oscillations and their temporal correlations on time scales of seconds to tens of seconds may be important for the temporal integrity of cognition (12). Higher cognitive functions, such as maintaining continuity of thoughts during rest, require causal sequences of neuronal activity, which may give rise to temporal correlations on multiple time scales. Interestingly, psychological and fMRI studies have pointed to prominent mnemonic activity during rest (1), and brain regions involved in mnemonic tasks (28, 35) overlap considerably with those showing high activity during rest (4). Thus, converging functional and anatomical evidence suggests that autocorrelated amplitude dynamics of temporo-parietal alpha oscillation and frontal theta during rest may be implicated in mnemonic processing and, therefore, not unexpectedly, affected in AD, as we have reported here.

Memory is believed to depend on the functional connectivity between different brain areas, and the cognitive symptoms of AD have therefore been proposed to reflect a "disconnection syndrome" (36). Indeed, there is considerable evidence pointing to deficits in the functional connectivity (7–9, 37–39), which may be related both to structural atrophy (28) and deficits in cholinergic or other neurotransmitter systems (18, 36, 40, 41). Failures in any of the components of a large-scale circuit are expected also to affect the temporal dynamics of local activity. It is therefore plausible that the abnormally weak correlations in alpha oscillations on time scales up to 25 s could in part be attributed to a "disconnection" in a large-scale network.

Our comparison of patient and control groups has provided fundamental insight into the pathophysiology of AD and indirect evidence for a functional role of stable oscillations in memory. In line with previously proposed neuroimaging biomarkers of early-stage AD (7), however, we found an overlap between the two subject groups. This is expected, because of the genetic variability of biomarkers: e.g., a subject with a genetic background causing a high DFA exponent of parietal alpha oscillations may fall outside the distribution of exponents for healthy subjects only in later stages of AD compared to a subject with a genetic background associated with a lower DFA exponent (22). In longitudinal studies, however, the heritability of biomarkers is expected to increase specificity and statistical power. We therefore propose that longitudinal mapping of the temporal structure of oscillations may prove valuable in preclinical trials aimed at investigating the progression and treatment response of patients with AD or other memory disorders (42).

Materials and Methods

Subjects. The study involved 19 patients [73.9 ± 6.4 years (mean ± standard deviation); 11 males] with a diagnosis of probable AD according to the

NINCDS-ADRDA criteria (43) and 16 healthy control subjects (70 ± 6.2 years; 7 males), i.e., with no known brain-related disorder. Patients and control subjects were recruited from the Alzheimer Center at the VU University Medical Center. Subjects were assessed according to a clinical protocol, which involved history taking, physical and neurological examination, blood tests, Mini–Mental State Examination (MMSE; total number of points = 30) (44), neuropsychological tests, and EEG. The final diagnosis was based upon a consensus meeting where all of the available clinical data and the results of the ancillary investigations were considered. Mean MMSE of patients was 21.3 (range: 14–28). Five controls were tested with MMSE (mean score 29, range: 26–30). Ten patients were taking cholinesterase inhibitors (7 patients were taking 24 mg/d galantamine and 3 patients were taking 12 mg/d rivastigmine. The same patients and MEG recordings were used in the study of Stam *et al.* (9). The study was approved by the Medical Ethical Committee of VU University Medical Center, and all patients or their caregivers had given written informed consent.

MEG Recording. Four minutes of data were acquired on a 151-channel MEG system (CTF Systems) at 625 Hz and band-pass filtered from 0.25 to 125 Hz. The subjects were comfortably seated and were instructed to close their eyes. The same acquisition settings were used for an empty-room recording without a subject in the MEG device to estimate the background noise of the laboratory.

Data Analysis. The recordings were down-sampled off-line to 125 Hz, high-pass filtered at 1 Hz and low-pass filtered at 45 Hz, using finite impulse response filters. The broadband data were visually inspected in segments of 5 seconds in the EEGLAB (45) data scroll viewer and segments containing non-periodic artifacts were marked and omitted from the analysis. Independent component analysis was performed with EEGLAB and components representing ECG, eye movements, or muscular artifacts were removed. Bad channels were repaired by replacing them with the average of their neighbors, and planar synthetic gradiometers (for two orthogonal directions giving 300 synthetic sensors) were computed using the Fieldtrip toolbox (http://www.ru.nl/fcdonders/fieldtrip/) and a method previously described (46). Planar synthetic gradiometers (for two orthogonal directions giving 300 synthetic sensors) were computed (46). The planar gradient fields are typically largest in magnitude directly above a given source (16, 46) and, therefore, provide an interpretation of topographic distributions that is analogous to projections of statistical maps onto the surface of the brain in PET and fMRI. The amplitude envelope of the oscillations was extracted using bandpass filters (finite impulse response filters with a Hamming window) and the Hilbert transform (Fig. 2*A* and *B*). The following filter settings were used (cut-off frequencies, filter order): delta (2–3 Hz, 251), theta (4–5 Hz, 63), alpha (6–13 Hz, 28), beta (15–25 Hz, 28), and gamma (30–45 Hz, 13). The mean oscillation amplitude was computed as the time-averaged amplitude envelope.

For each synthetic sensor and subject, we computed the median amplitude and used this as the threshold for defining the beginning and the end of an oscillation burst. The periods of the amplitude envelope remaining above and below this median level were termed life- and waiting-times, respectively (Fig. 2*A*). Probability distributions of life- and waiting-times were initially computed using equidistant binning on a logarithmic axis with 10 bins per decade. Based on visual inspection of probability distributions in the alpha band from MEG channels in the parietal region, which have a high signal-to-noise ratio, it was found that both subject groups had probability distributions that decayed slowly compared to those of the empty-room recording or temporally uncorrelated signals that were filtered and analyzed identically to the MEG signals with a subject in the scanner (Fig. S1 *C* and *D*). We computed the cumulative probability distributions and extracted the 95th percentile (Fig. 2 *H* and *I*; Fig. S1 *E* and *F*) as a quantitative index of the fat-tailed probability distributions of life- and waiting-times in a given sensor location and frequency band (Fig. 2 *F* and *G*; Fig. S1 *C* and *D*). We refer to the 95th percentiles as ''life- and waiting-time biomarkers.'' It is possible that the reported alteration in the temporal dynamics of ongoing oscillations in the AD patients can be detected also with other time series methods.

The threshold was based on local properties of the signal (the median in individual sensors), because large differences in asynchronous background MEG and, potentially, differences between sources and sensors make it impossible to define an absolute threshold that can be used across all subjects and sensors. To test whether our main result was sensitive to changes in the relative threshold, we repeated the analysis in the alpha band using thresholds of 25% above and below the median level (Fig. S4 *A* and *B*). These changes naturally affect the exact estimates of individual oscillation-burst life-times, however, topographic differences between the patients and the control group were strikingly similar for the three different thresholds (Fig. S4). In contrast, the use of an absolute threshold (the median level in a parietal sensor from subject 1) resulted in the problem that different subjects and different channels were considered to have no oscillations, which makes it impossible to perform a statistical analysis of the two subject groups.

The DFA was used to analyze the decay of temporal (auto)correlations in the time range of 1–25 s, also known as long-range temporal correlations (LRTC). The DFA was introduced as a method to quantify correlations in complex data with less strict assumptions about the stationarity of the signal than the classical autocorrelation function or power spectral density (47). An additional advantage of DFA is the greater accuracy in the estimates of correlations, which facilitates a reliable analysis of LRTC up to time scales of at least 10% of the duration of the signal (22, 48). The main steps from the broadband MEG signal to the quantification of LRTC using DFA have been explained in detail elsewhere (23, 49, 50). In brief, the DFA measures the scaling of the root-mean-square fluctuation of the integrated and linearly detrended signals, $F(t)$, as a function of time window size, t (Fig. 2 *J* and Fig. S1*G*). The DFA exponent is the slope of the fluctuation function shown in Fig. 2 *J*. A larger DFA exponent in the interval of 0.5 to 1.0 indicates a greater persistence of temporal correlations (stronger autocorrelations), whereas an uncorrelated signal is characterized by an exponent of 0.5.

Statistical Analysis. The biomarker value in each channel was computed as the average across the two orthogonal synthetic sensors. Two-tailed *t*-tests between patient and control groups were performed; *P*-values below 0.05 and 0.01 are indicated on topographic plots. A correction for multiple comparisons was not necessary, because the number of channels with *P*-values below 0.05 ranged from 13 and 38 and the likelihood of having this many channels out of 150 by chance is less than 2% (*cf.* binomial distribution). Furthermore, the channels were anatomically clustered in the topographic plots (Fig. 3). Biomarker values of patient and control groups are reported as mean ± standard error of mean (SEM) based on the average values across channels with $P < 0.05$ in the initial two-tailed *t* test. Group differences in these cross-channel means were computed using the two-tailed *t* test.

ACKNOWLEDGMENTS. 'T.M. received funding from Fundação para a Ciência e a Tecnologia (FCT), Ministry of Science, Portugal and the Calouste Gulbenkian Foundation. S.-S.P. received funding from the Toptalent program of the Netherlands Organization for Scientific Research (NWO). K.L.-H. received funding from the Danish Research Agency and the Innovative Research Incentive Schemes of the NWO.

1. Binder R, *et al.* (1999) Conceptual processing during the conscious resting state: a functional MRI study. *J Cognit Neurosci* 11:80–93.
2. Mason MF, *et al.* (2007) Wandering minds: the default network and stimulus-independent thought. *Science* 315:393–395.
3. Smallwood J, Schooler JW (2006) The restless mind. *Psycholl Bull* 132:946–958.
4. Fox MD, Raichle ME (2007) Spontaneous fluctuations in brain activity observed with functional magnetic resonance imaging. *Nat Rev Neurosci* 8:700–711.
5. Damoiseaux JS, *et al.* (2006) Consistent resting-state networks across healthy subjects. *Proc Natl Acad Sci USA* 103:13848–13853.
6. Gusnard DA, Raichle ME (2001) Searching for a baseline: functional imaging and the resting human brain. *Nat Rev Neurosci* 2:685–694.
7. Greicius MD, Srivastava G, Reiss AL, Menon V (2004) Default-mode network activity distinguishes Alzheimer's disease from healthy aging: evidence from functional MRI. *Proc Natl Acad Sci USA* 101:4637–4642.
8. Babiloni C, *et al.* (2004) Abnormal fronto-parietal coupling of brain rhythms in mild Alzheimer's disease: a multicentric EEG study. *Eur J Neurosci* 19:2583–2590.
9. Stam CJ, *et al.* (2006) Magnetoencephalographic evaluation of resting-state functional connectivity in Alzheimer's disease. *NeuroImage* 32:1335–1344.
10. Greicius MD, *et al.* (2007) Resting-state functional connectivity in major depression: abnormally increased contributions from subgenual cingulate cortex and thalamus. *Biol Psych* 62:429–437.
11. Buckner RL, Andrews-Hanna JR, Schacter DL (2008) Anatomy, function, and relevance to disease. *Ann NY Acad Sci* 1124:1–38.
12. Linkenkaer-Hansen K, *et al.* (2005) Breakdown of long-range temporal correlations in theta oscillations in patients with major depressive disorder. *J Neurosci* 25:10131–10137.
13. Cowan N (1998) Visual and auditory working memory capacity. *Trends Cogn Sci* 2:77–77.
14. Raghavachari S, *et al.* (2001) Gating of human theta oscillations by a working memory task. *J Neurosci* 21:3175–3183.
15. Jensen O, Gelfand J, Kounios J, Lisman JE (2002) Oscillations in the alpha band (9–12 Hz) increase with memory load during retention in a short-term memory task. *Cereb Cortex* 12:877–882.
16. Jokisch D, Jensen O (2007) Modulation of gamma and alpha activity during a working memory task engaging the dorsal or ventral stream. *J Neurosci* 27:3244–3251.
17. Jeong J (2004) EEG dynamics in patients with Alzheimer's disease. *Clin Neurophysiol* 115:1490–1505.

18. Osipova D, *et al.* (2005) Altered generation of spontaneous oscillations in Alzheimer's disease. *NeuroImage* 27:835–841.
19. Fernandez A, *et al.* (2002) Focal temporoparietal slow activity in Alzheimer's disease revealed by magnetoencephalography. *Biol Psych* 52:764–770.
20. Harris TE (2002) *The Theory of Branching Processes* (Courier Dover Publications, New York).
21. Plenz D, Thiagarajan TC (2007) The organizing principles of neuronal avalanches: cell assemblies in the cortex? *Trends Neurosci* 30:101–110.
22. Linkenkaer-Hansen K, *et al.* (2007) Genetic contributions to long-range temporal correlations in ongoing oscillations. *J Neurosci* 27:13882–13889.
23. Linkenkaer-Hansen K, Nikouline VV, Palva JM, Ilmoniemi RJ (2001) Long-range temporal correlations and scaling behavior in human brain oscillations. *J Neurosci* 21:1370–1377.
24. Beran J (1994) *Statistics for Long-Memory Processes* (Chapman & Hall/CRC, Palm Beach).
25. Poil S-S, van Ooyen A, Linkenkaer-Hansen K (2008) Avalanche dynamics of human brain oscillations: relation to critical branching processes and temporal correlations. *Hum Brain Mapp* 29:770–777.
26. Monto S, Vanhatalo S, Holmes MD, Palva JM (2007) Epileptogenic neocortical networks are revealed by abnormal temporal dynamics in seizure-rree subdural EEG. *Cereb Cortex* 17:1386–1393.
27. Parish LM, *et al.* (2004) Long-range temporal correlations in epileptogenic and non-epileptogenic human hippocampus. *Neuroscience* 125:1069–1076.
28. Buckner RL (2004) Memory and executive function in aging and AD: multiple factors that cause decline and reserve factors that compensate. *Neuron* 44:195–208.
29. Johannsen P, Jakobsen J, Gjedde A (2000) Statistical maps of cerebral blood flow deficits in Alzheimer's disease. *Eur J Neurol* 7:385–392.
30. Thompson PM, *et al.* (2003) Dynamics of gray matter loss in Alzheimer's disease. *J Neurosci* 23:994–1005.
31. Gevins A (1997) High-resolution EEG mapping of cortical activation related to working memory: effects of task difficulty, type of processing, and practice. *Cereb Cortex* 7:374–385.
32. Bressler SL, Tognoli E (2006) Operational principles of neurocognitive networks. *Int J Psychophysiol* 60:139–148.
33. Honey CJ, Kotter R, Breakspear M, Sporns O (2007) Network structure of cerebral cortex shapes functional connectivity on multiple time scales. *Proc Natl Acad Sci USA* 104:10245.
34. Nikouline VV, Linkenkaer-Hansen K, Huttunen J, Ilmoniemi RJ (2001) Interhemispheric phase synchrony and amplitude correlation of spontaneous beta oscillations in human subjects: a magnetoencephalographic study. *NeuroReport* 12:2487–2491.
35. Kuhl BA, Dudukovic NM, Kahn I, Wagner AD (2007) Decreased demands on cognitive control reveal the neural processing benefits of forgetting. *Nat Neurosci* 10:908–914.
36. Delbeuck X, Van der Linden M, Collette F (2003) Alzheimer' disease as a disconnection syndrome? *Neuropsych Rev* 13:79–92.
37. Rombouts SA, *et al.* (2005) Altered resting state networks in mild cognitive impairment and mild Alzheimer's disease: an fMRI study. *Hum Brain Mapp* 26:231–239.
38. Lustig C, *et al.* (2003) Functional deactivations: change with age and dementia of the Alzheimer type. *Proc Natl Acad Sci USA* 100:14504–14509.
39. Stam CJ, *et al.* (2005) Disturbed fluctuations of resting state EEG synchronization in Alzheimer's disease. *Clin Neurophysiol* 116:708–715.
40. Osipova D, *et al.* (2003) Effects of scopolamine on MEG spectral power and coherence in elderly subjects. *Clin Neurophysiol* 114:1902–1907.
41. Maxim V, *et al.* (2005) Fractional Gaussian noise, functional MRI and Alzheimer's disease. *NeuroImage* 25:141–158.
42. Thal LJ, *et al.* (2006) The role of biomarkers in clinical trials for Alzheimer disease. *Alzheimer Dis Assoc Disord* 20:6–15.
43. McKhann G, *et al.* (1984) Clinical diagnosis of Alzheimer's disease: Report of the NINCDS-ADRDA Work Group under the auspices of Department of Health and Human Services Task Force on Alzheimer's Disease. *Neurology* 34:939–944.
44. Folstein MF, Folstein SE, McHugh PR (1975) ''Mini-mental state'': a practical method for grading the cognitive state of patients for the clinician. *J Psych Res* 12:189–198.
45. Delorme A, Makeig S (2004) EEGLAB: an open source toolbox for analysis of single-trial EEG dynamics including independent component analysis. *J Neurosci Meth* 134:9–21.
46. Bastiaansen MCM, Knosche TR (2000) Tangential derivative mapping of axial MEG applied to event-related desynchronization research. *Clin Neurophysiol* 111:1300–1305.
47. Peng CK, *et al.* (1994) Mosaic organization of DNA nucleotides. *Physical Review E Stat Phys Plasmas Fluids Relat Interdiscip Topics* 49:1685–1689.
48. Gao J, *et al.* (2006) Assessment of long-range correlation in time series: how to avoid pitfalls. *Physical Review E Stat Nonlin Soft Matter Phys* 73:016117.
49. Linkenkaer-Hansen K, *et al.* (2004) Stimulus-induced change in long-range temporal correlations and scaling behaviour of sensorimotor oscillations. *Eur J Neurosci* 19:203–218.
50. Nikulin VV, Brismar T (2005) Long-range temporal correlations in electroencephalographic oscillations: relation to topography, frequency band, age and gender. *Neuroscience* 130:549–558.